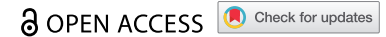


RESEARCH ARTICLE



Long-term stability and immunogenicity of lipid nanoparticle COVID-19 mRNA vaccine is affected by particle size

Ruimeng Shi^a, Xueli Liu^b, Yajuan Wang^c, Meilu Pan^b, Shaoqin Wang^a, Lin Shi^b, and Beibei Ni^c

^aSchool of Pharmacy, Hebei Medical University, Shijiazhuang, PR China; ^bPharmacology Laboratory, Hebei Research Institute of Pharmaceutical and Medical Device Inspection, Shijiazhuang, PR China; ^cResearch and Development Department, CSPC Pharmaceutical Group Co., Ltd., Shijiazhuang, PR China

ABSTRACT

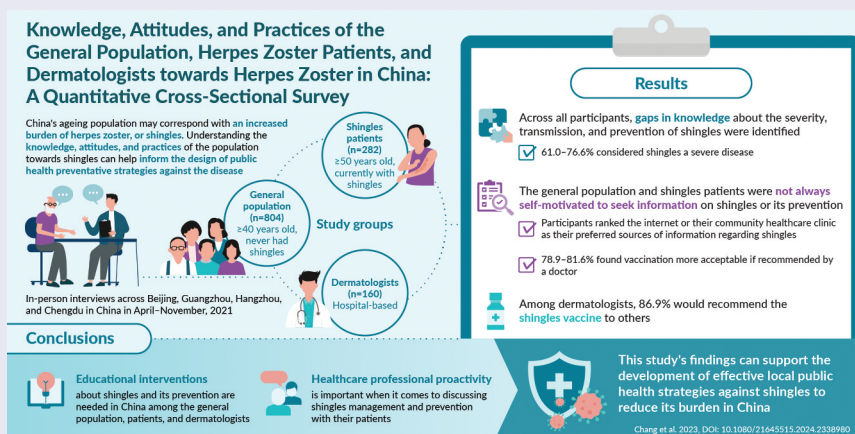
Messenger ribonucleic acid (mRNA) technology has been rapidly applied for the development of the COVID-19 vaccine. However, naked mRNA itself is inherently unstable. Lipid nanoparticles (LNPs) protect mRNAs from extracellular ribonucleases and facilitate mRNA trafficking. For mRNA vaccines, antigen-presenting cells utilize LNPs through uptake to elicit antigen-specific immunity. There are reports on the impact of various physical characteristics of LNPs, particularly those with sizes less than 200 nm, especially 50 to 150 nm, on the overall stability and protective efficacy of mRNA vaccines. To address this, a single change in the size of LNPs using the same mRNA stock solution was assessed for the physicochemical characterization of the resulting mRNA-LNPs vaccine, along with the evaluation of their protective efficacy. Particles of smaller sizes generally disperse more effectively in solutions, with minimized occurrence of particle precipitation and aggregation. Here, we demonstrate that the vaccine containing 80–100 nm mRNA-LNPs showed the best stability and protection at 4°C and –20°C. Furthermore, we can conclude that freezing the vaccine at –20°C is more appropriate for maintaining stability over the long term. This effort is poised to provide a scientific basis for improving the quality of ongoing mRNA vaccine endeavors and providing information on the development of novel products.

ARTICLE HISTORY

Received 29 November 2023
Revised 22 March 2024
Accepted 9 April 2024

KEYWORDS



mRNA vaccine; SARS-CoV-2; lipid nanoparticle; particle size; stability; biological activity



Introduction

Messenger RNA (mRNA) vaccines have been pioneers in the fight against coronavirus disease, 2019 (COVID-19). mRNA vaccines offer advantages compared to traditional recombinant protein vaccines, inactivated vaccines, and attenuated vaccines, such as fast production speed, simplified preparation, robust antibody responses, prolonged immunity, and improved safety.^{1,2} The mRNA-lipid nanoparticles (LNPs) platform is an effective tool for delivering messenger mRNA in the body for prophylactic and therapeutic purposes.³ Besides, LNPs are highly promising carriers for a diverse array of therapeutic agents and have garnered

significant attention in the pharmaceutical industry over recent years.⁴ LNPs play a pivotal role in the efficient delivery and promotion of antigen expression for mRNA vaccinespecific antibody responses.^{4,12 5–714} Especially in the current context, vaccines are crucial tools in combating the COVID-19 pandemic, and LNPs serve as pivotal components of mRNA vaccines.^{8,15} mRNA vaccine technology has been applied to a variety of infectious diseases, such as mRNA vaccines are already in clinical studies for the prevention of viruses like HIV-1, chikungunya, Zika, and influenza.^{2,9–115,16–18} In addition, two mRNA vaccines against COVID-19 developed by Pfizer-BioNTech and Moderna have been approved for clinical use in adults aged 65 years and

CONTACT Xueli Liu  xueli2019@hotmail.com  Pharmacology Laboratory, Hebei Research Institute of Pharmaceutical and Medical Device Inspection, No. 219 Yuquan Road, Shijiazhuang 050227, PR China.

 Supplemental data for this article can be accessed on the publisher's website at <https://doi.org/10.1080/21645515.2024.2342592>

© 2024 The Author(s). Published with license by Taylor & Francis Group, LLC.

This is an Open Access article distributed under the terms of the Creative Commons Attribution-NonCommercial License (<http://creativecommons.org/licenses/by-nc/4.0/>), which permits unrestricted non-commercial use, distribution, and reproduction in any medium, provided the original work is properly cited. The terms on which this article has been published allow the posting of the Accepted Manuscript in a repository by the author(s) or with their consent.

older, with efficacy rates of more than 95% and 94%, respectively. The CSPC Group (CSPC Holdings Company Limited) announced the inclusion of its novel coronavirus mRNA vaccine (SYS6006) for emergency use in China, with now completed Phase I, Phase II, and sequential booster immunization clinical studies.^{12,13,19,20} These accomplishments underscore that the technological avenue involving LNP-mediated delivery of mRNA vaccines has materialized as an effective approach for the prevention of COVID-19.^{14,21} To generate liquid mRNA, it is essential to maintain a sterile environment and adhere to rigorous quality control protocols at every stage of the production process to guarantee the safety and efficacy of the end product. Although mRNA vaccines have become a global technology, their comprehensive understanding is still lacking at home and abroad. Among these, the average particle size and distribution of LNPs are the key factors determining the quality of LNPs and their suitability for various applications.^{15,22} Generally, the optimal size for LNPs is in the range of 20 to 200 nm. This range ensures the stability of LNPs in fluids like blood and lymph while facilitating interstitial penetration.^{16,17,23} Considering this, we embarked on a thorough investigation focusing on LNPs of varying sizes within the narrower range of 60 to 150 nm. To specifically investigate the role of particle size in vaccine efficacy, all other aspects of the mRNA vaccine must be matched. Here, we single-varied the size of mRNA-LNPs of COVID-19 vaccine independent of lipid composition and systematically investigated the size possessing optimal long-term stability with bioprotective properties.

While the *in vivo* safety and efficacy of mRNA-LNPs vaccines have considerably progressed through both domestic and international research, the focus on the stability of vaccines with varying particle sizes during storage is notably constrained.^{16,24} Furthermore, our understanding of the structure and morphology of LNPs encapsulating mRNA, the necessity of electron microscopy, the chemical stability of the constituents of LNPs, and the overall colloidal stability of the mRNA-LNPs system remains relatively limited.^{17,18,25,26} As mRNA is inherently an active pharmaceutical molecule, robust encapsulation of mRNA payload (>80%) within the lipid shell of LNPs is essential for ensuring the stability and effectiveness of mRNA-LNPs vaccines. Monitoring the physicochemical attributes, encapsulation efficiency, integrity, and lipid content of mRNA-LNPs is imperative.^{19–21,27–29} In this study, mRNA-LNPs vaccines with size variations (80–150 nm) were prepared without changing the lipid composition of LNPs. Additionally, 60–80 nm LNPs (without messenger mRNA) were also prepared. In addition, crucial physicochemical properties of the vaccines stored at different temperatures and durations were examined by employing relevant *in vivo* bioactivity assays for the prepared vaccine formulations.^{22,30} Throughout this research endeavor, we carefully observed and monitored the compositional changes of mRNA-LNPs stored for different durations in accelerated experimental conditions at 4°C and frozen at –20°C. The goal was to explore the differences in long-term stability and protective efficacy of fully formed mRNA-LNPs vaccine formulations of varying sizes prepared from the same mRNA stock solution. In the future, a theoretical and experimental basis is anticipated to be established to facilitate the creation of the most effective mRNA vaccine to combat COVID-19 infection, thus paving the way for further research into novel coronavirus vaccine prophylaxis and treatments.

Materials and methods

Materials

SM-102 (heptadecan-9-yl 8-((2-hydroxyethyl)(6-oxo-6-(undecyloxy) hexyl) amino) octanoate) and 1,2-dimyristoyl-rac-glycerol-3-methoxy poly ethylene glycol-2K (mPEG-DMG-2K) were obtained from Xiamen Sinopeg Biotech Co., Ltd. located in Xiamen, China. The lipid 1,2-distearoyl-sn-glycerol-3-phosphocholine (DSPC) was acquired from Lipoid GmbH in Ludwigshafen, Germany. Cholesterol was obtained from Nippon FINE Chemical Co., Ltd. Sodium chloride, sucrose, sodium acetate trihydrate, and tris(hydroxymethyl) methyl aminomethane (Tris) were obtained from Merck in Darmstadt, Germany. Citric acid was purchased from Hunan Erkang Pharmaceutical Co., Ltd. in Hunan, China. Mouse IFN γ , IL-4 ELISA Kit was obtained from Thermo Fisher Scientific Co., Ltd. in Beijing, China.

Production of mRNA-LNPs

The lipids (including SM-102, DSPC, cholesterol, and mPEG-DMG-2K) were dissolved in ethanol at a molar ratio of 50:10:38.5:1.5 to prepare the lipid fraction. The aqueous mRNA phase was prepared by dissolving the mRNA stock solution in pH 4.0 buffer containing citric acid and sodium chloride. The lipid and mRNA aqueous phases were mixed at a flow rate ratio of 1:3 (amine-to-phosphate ratio (N/P) of 6) using a T-joint mixer. The diafiltration Volume method keeps the permeate flow rate and the buffer make-up rate equal, the material volume constant, the exudate volume constant, and the inlet pressure at 0.5 bar. When the buffer volume equals the sample volume (300 mL), the diafiltration Volume process is one-time (the buffer makeup and the material volume are equal to represent 1 diafiltration Volume). For 60–80 nm LNPs, the resulting mixture will be 8 diavolumes in pH 7.4 buffer (containing 20 mM Tris, 10.7 mM sodium acetate, and 8.7% sucrose); 80–100 nm mRNA-LNPs in pH 7.4 Buffer for 8 diavolumes; For samples that require a two-step diavolumes, the 100–120 nm mRNA LNPs are first treated with 3 diavolumes in pH 4.0 buffer (citric acid and sodium chloride) and then 5 diavolumes in pH 7.4 buffer; For the preparation of 120–150 nm mRNA-LNPs, firstly the mixture was treated with 5 diavolumes in pH 7.4 buffer. In the second step the resulting mixture was subjected to 3 diavolumes using pH 4.0 buffer as well as 3 diavolumes using pH 7.4 buffer, the resulting mixture was repeated in the second step to finally produce 120–150 nm mRNA-LNPs. All four vaccine groups were treated with diavolumes in pH 7.4 buffer to increase the vaccine pH. Consequently, the vaccine formulations contained only the pH 7.4 Tris buffer. The preparation process is shown in Table S1. The particle size of the LNPs was increased by repeated diafiltration volume.

Monitoring physical and chemical characterization of mRNA-LNPs

The size of the mRNA LNPs before stability and immunogenicity studies is crucial for experimental purposes, so we used cryo-electron microscopy (Cryo-TEM) to observe the structure of the samples in their original state, and dynamic light scattering (DLS) to determine the average particle size of the characterized

preparations along with their distribution frequency, and screen vaccines that meet the size requirements.

Set time points (0,1,2,3,4,5, and 6 months or 3,6,9, and 12 months), the test vials were removed from the refrigerator and allowed to return to room temperature. The mRNA-LNPs were transferred to polystyrene cuvettes, and a Malvern (Model number, Nano ZS) particle size analyzer was used to measure their particle size and polydispersity index. The parameters used included a dispersant (8.7% sucrose), a temperature of 25°C, and an equilibration time of 120 s.

We weighed 0.24 g of trometamol, 0.146 g of trisodium citrate dihydrate, and 8.7 g of sucrose (Merck), and dissolved them in water in a 100 mL volumetric flask to create a dispersant. The pH was adjusted to 7.4 by adding 0.5 mL of hydrochloric acid (2 mol/L). Then, 50 µL of the test samples were added to 1450 µL of the dispersant and mixed thoroughly; two parallel batches of the formulation were prepared. The parameters were set and Zeta potential was measured for the formulation.

The lipid content was analyzed using an ultra-high-performance liquid chromatography (UHPLC) system with a charged aerosol detector (CAD). The UHPLC method utilized a C18-bonded silica gel column (Chrom Core 300 C-18, 4.6 × 250 mm, 5 µm) with the mobile phase of 0.5 g/L ammonium acetate in methanol. The flow rate was set at 1 mL/min. For the analysis, 300 µL of the mRNA-LNPs sample was mixed with 900 µL of anhydrous ethanol as the test solution. Reference solutions for each of the four lipid fractions (including SM-102, DSPC, cholesterol, and mPEG-DMG-2K) were prepared for subsequent lipid content calculations. The linear regression equation was calculated using the logarithmic values of the concentration of the serial control solution and the logarithmic value of the corresponding peak area.

$$\ln A1 = a \times \ln C + b \text{MOI}\% = \frac{e^{[(\ln A2 - b)/a] \times E}}{D} \times 100\%$$

A1: Peak area of each lipid in each control solution; C: Concentration of each lipid in each control solution, mg/mL; a: slope of the standard curve; b: intercept of the standard curve; A2: Peak area of each lipid in the test solution; E: dilution of the test sample; D: labeled amount. The labeling amount of SM-102, cholesterol, DSPC, and mPEG-DMG-2K was 1.27 mg/mL in the following order, 0.53 mg/mL, 0.28 mg/mL, 0.14 mg/mL.

RiboGreen, a fluorescent dye, was used for detecting RNA content in solutions. When mixed directly with the formulation sample, RiboGreen can detect the amount of free RNA. The permeability of lipid particles in the formulation sample was increased through the addition of 10% Triton X-100 (Sigma), and the sample can be assessed for total RNA content by binding it with RiboGreen (Thermo Scientific). For the procedure, 100 µL of the sample was diluted 50 times with 1× TE buffer, and prepared in duplicates for both the A and B formulations. Negative controls A and B were also prepared using the above samples. All samples (100 µL) were added to separate wells of a black-bottom 96-well plate. Each sample was prepared in duplicates, and 100 µL of RNA reagent was added, mixed, and shaken for 2 min. The excitation and emission wavelengths were set to 480 nm and 520 nm, respectively.

The Agilent 2100 Bioanalyzer is a platform based on the capillary electrophoresis principle, utilizing microfluidic chips to separate and detect mRNA. RNA purity is estimated based on the peak area (time-corrected area); the peak areas of all peaks except the internal standard peak, were added to obtain the total peak area. The ratio of the main peak area to the total peak area represents the purity of the mRNA in the original solution. The purity for the three replicates from each batch of the original solution was calculated, and the average value was taken as the purity of the original RNA. The incomplete RNA content was calculated as 100% minus the RNA purity percentage.

Animal experimentation groups and immunization protocol

Immunogenicity of mRNA-LNPs vaccine in female BALB/c mice (6–8 weeks old) were injected intramuscularly with fresh mRNA-LNPs or stored for 3 and 6 months at 4°C (5 µg, *n* = 8). Each test preparation group was given 0.9% saline as a control. All groups followed the same immunization procedure and used the same positive control serum for each ELISA experiment (see Table S2-S3). All mice were injected with the same booster dose 7 days after the initial vaccination. Mice were immunized twice at 7 days (0–7 days) and 21 days (0–21 days), and serum samples were collected sequentially after the last immunization to determine the titer of antigen S protein-binding antibodies. The results showed that the serum binding antibodies showed consistent changes at different immunization intervals (see Figure S1-S2). Mice were anesthetized using isoflurane, and blood was collected through the retro-orbital route. The serum was separated from blood by centrifugation at 3000 g for 10 min, and stored at –80°C until further use.

Enzyme-linked immunosorbent assay measurement of antibody and cytokine levels in the serum

Serum antibodies

For ELISA, a 96-well ELISA microplate was coated with 2 ng/µL of S protein (GenScript) in coating buffer (1× phosphate buffered saline) and incubated overnight at 4°C. The wells were washed and blocked, and then serially diluted mouse sera were added and incubated at 37°C for 2 h. Following this, the diluted goat anti-mouse IgG secondary antibody (1:10000, SinoBio) was added. The antibody reaction was detected using 3'5'-tetramethylbenzidine (TMB, Solarbio) as the substrate and 1 M H₂SO₄ as the stop solution. Cytokine interleukin 4 (IL-4) and interferon-gamma (IFN-γ) assay kit instructions (eBioscience ELISA). The total levels of IgG1 and IgG2a were assessed using ELISA kits (Solarbio). The absorbance was measured at 450 nm, and the data were fitted to a dose–response four-parameter logistic model.

Statistical analysis

Statistical significance was calculated across groups by two-way analysis of variance and multiple comparisons using GraphPad Prism 9.0. The *p*-value <.05 between the two groups was considered statistically significant.

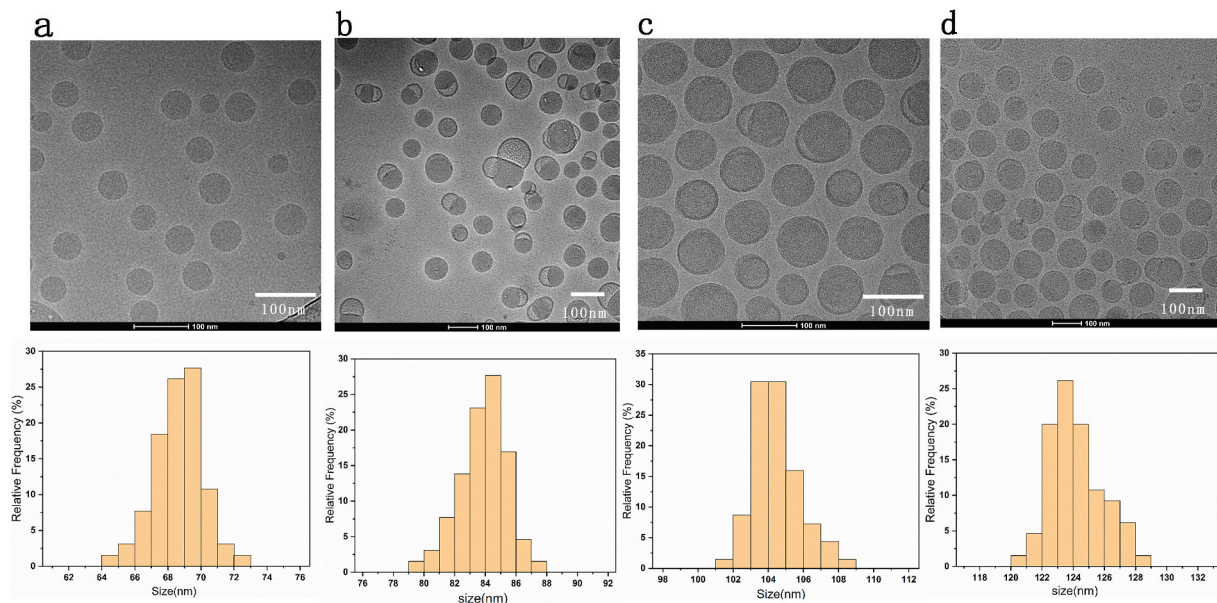


Figure 1. (a) The Cryo-TEM images and DLS particle size distribution of 60–80 nm (LNPs without encapsulated mRNA) (b–d) Cryo-TEM images and DLS particle size distribution of 80–100 nm, 100–120 nm, 120–150 nm mRNA-LNPs. Histogram of the mean particle size of the four groups of samples. Frequency count analysis of particle size data using the Origin 2019 software, each sample is an average of at least 30 readings. Scale = 100 nm.

Results

(Figure 1(a)) 60–80 nm LNPs were mainly distributed in the range of 64–73 nm interval, concentrated between 68–71 nm; (Figure 1(b)) 80–100 nm mRNA-LNPs were distributed in 79–88 nm, concentrated between 82–86 nm; (Figure 1(c)) 100–120

nm mRNA-LNPs were distributed in 101–109 nm, concentrated between 103–107 nm; (Figure 1(d)) 120–150 nm mRNA-LNPs were distributed in 122–126 nm with uniform distribution. In addition, after treatment with 8 diavolumes, the ethanol residue was close to 0 (see Table S4 for more details about the results). Collecting the characterization information of Cryo-TEM images,

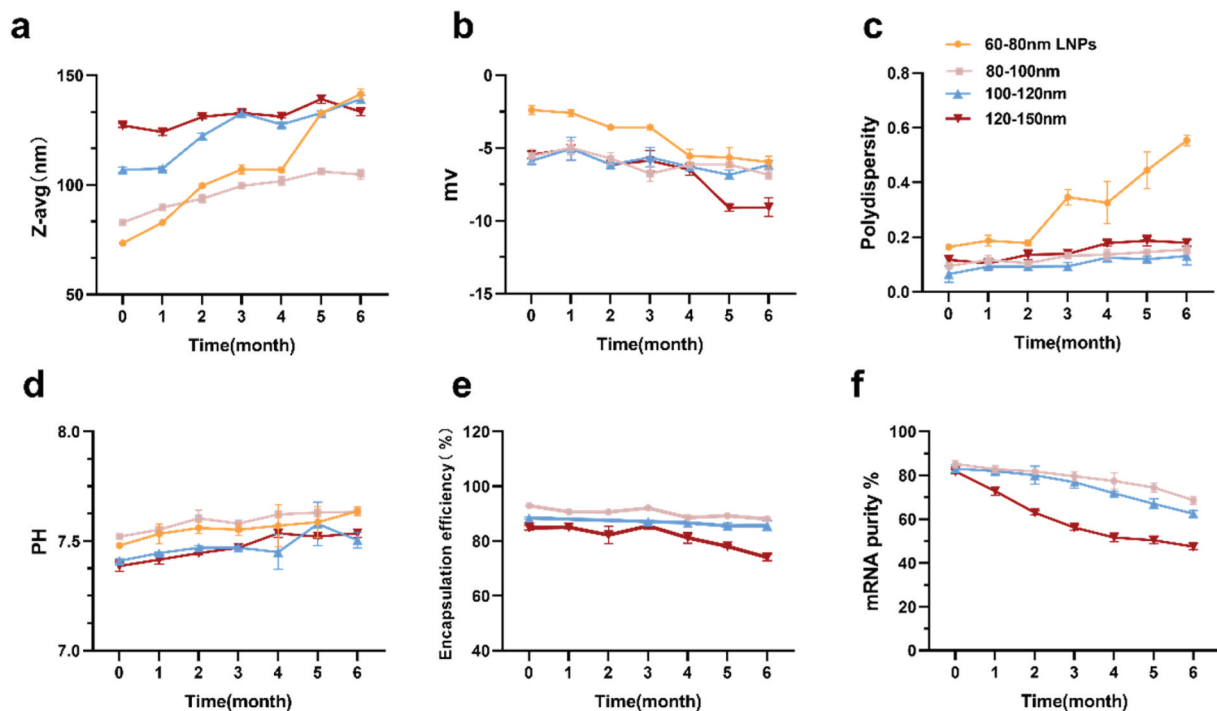


Figure 2. Analytical testing of the physicochemical properties of mRNA-lipid nanoparticles (LNPs) stored at 4°C for 6 months. (a) Particle size, (b) Zeta potential using electrophoretic light scattering, and (c) polydispersity were measured by dynamic light scattering, (d) determination of pH, (e) mRNA encapsulation determined by RiboGreen assay, while (f) mRNA purity was assessed by capillary electrophores. For (a) (b) (c) and (d), each data point is an average of at least 10 readings, resulting in the mean z-average, polydispersity, zeta potential, and pH values, which are displayed on the graphs. Analyses in (e)–(f) were done in triplicate. Error bars represent the standard deviation.

we conclude that prepared vaccine samples are within particle size requirements. Can be used for subsequent stability and immunogenicity studies.

Physicochemical characterization of mRNA-LNPs at 4°C in accelerated experiments

We observed that after 3 and 6 months of storage of four groups of preparations at 4°C, the average particle sizes remained below 150 nm (Figure 2(a)). In contrast, the particle size of 60–80 nm LNPs (LNPs without encapsulated mRNA) increased by nearly 150 nm after 6 months of storage, with a 96.79% increase in its average particle size. The groups with 80–100 nm and 100–120 nm particle sizes showed a significant increase from 0 to 3 months, and a gradual slowdown between 3 to 6 months. In addition, as shown in Figure 2(b), the PDI dispersion coefficients of the four groups of preparations showed an increasing tendency to varying degrees. The PDI coefficients of 60–80 nm LNPs had the same outliers, far beyond our required range (PDI <0.3). The stability of 60–80 nm LNPs was greatly affected after 6 months of storage at 4°C. The pH of the four groups of preparations did not change significantly and remained between 7.4 and 7.6, all within a reasonable range (Figure 2(c)). The three groups of vaccine preparations exhibited no significant change in zeta charge when stored for up to 3 months (Figure 2(d)). When stored for up to 6 months, the potential of the vaccine from the 120–150 nm mRNA-LNPs group decreased significantly and showed a more negative trend compared to the other two groups.

At 4°C for 3 months, the decrease in the encapsulation efficiency of the three groups of mRNA-LNPs was not significant (Figure 2(e)). However, when stored for up to 6 months, the encapsulation rate of 120–150 nm mRNA-LNPs products decreased steadily. The mRNA purity of nucleoside-modified mRNA-LNPs was determined by capillary electrophoresis.

Changes in the mRNA purity of the three groups of mRNA vaccines were significant in non-frozen products stored at 4°C for at least 6 months (Figure 2(f)). The mRNA integrity of the 120–150 nm mRNA-LNPs stored at 4°C for 6 months decreased by approximately 25%–30%. Meanwhile, there was about a 15% decrease in mRNA integrity of the 100–120 nm mRNA vaccines, while the least loss of mRNA integrity was observed in the 80–100 nm mRNA-LNPs. Overall, these results demonstrate a superior stability of the 80–100 nm mRNA-LNPs compared to the other two groups of mRNA-LNPs.

Based on the above results, we speculated whether the degradation of lipid components might have led to altered physicochemical properties. Considering that in LNPs, each lipid component plays a specific role in the formation, stability, and biological properties of the particle, we performed UHPLC analysis. In this comprehensive study, the stability of mRNA-LNPs vaccines formulated in the liquid state was determined when stored at 4°C for 6 months. The particle characteristics of the four groups of lipid components in the non-frozen vaccine formulations showed significant changes (Figure 3). The lipid components of the 120–150 nm mRNA-LNPs vaccine exhibited significant degradation after 6 months of storage; in contrast, the vaccine from the 80–100 nm mRNA-LNPs showed the lowest degree of degradation among the four lipid components, indicating better stability compared to the vaccine from the other two groups. The lipid components of the vaccine from the 100–120 nm mRNA-LNPs group exhibited degradation levels between the other two vaccines.

Long-term protective efficacy of mRNA-LNPs under 4°C refrigeration

Following the second immunization, the antibody titers observed at three-time points (0, 3, and 6 months after

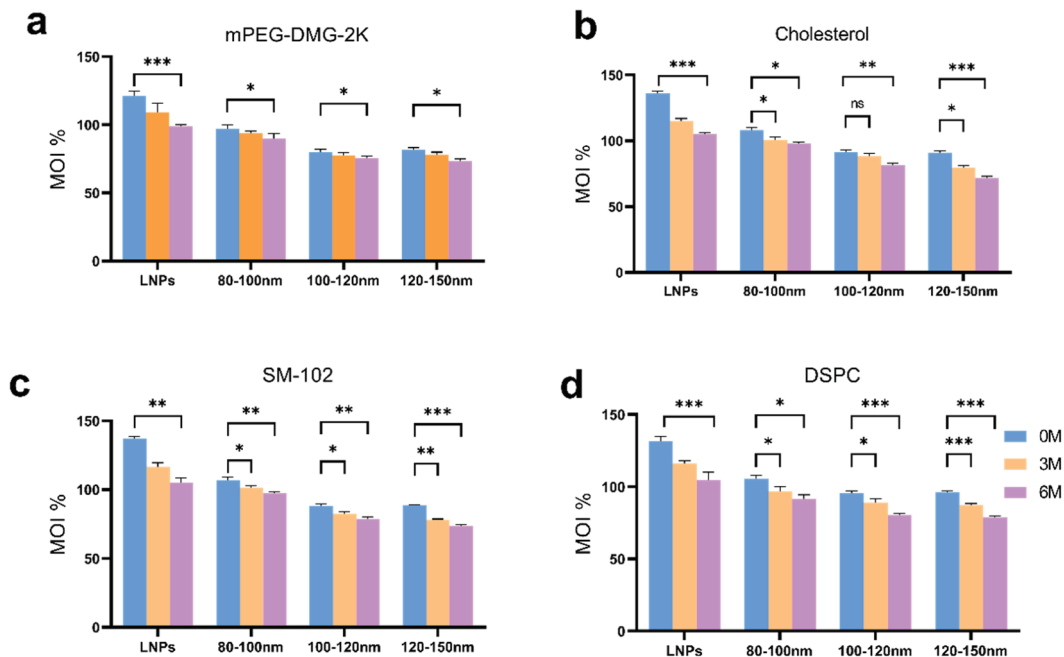


Figure 3. Ultra-high performance liquid chromatography (UHPLC) analysis of four lipid components of mRNA-LNPs. (a) Differences in changes of mPEG-DMG-2K in formulation stored at 4°C for 0, 3, and 6 months. (b) Differences in changes in cholesterol of the fractions after 0, 3 and 6 months of storage at 4°C. (c) Analysis of lipid content of the ionizable lipid (SM-102) in formulation fractions of different particle sizes. (d) Analyze differences in changes in DSPC after 0, 3 and 6 months of storage at 4°C. Calculations are described in the ‘Lipid Content Determination’ section of materials and methods. MOI%: the percentage of lipid content detected in the sample as a percentage of the labeled amount. Data were analyzed by a two-tailed unpaired t-test. * $P < .05$, ** $P < .01$, *** $P < .001$. All panels were analyzed in triplicate.

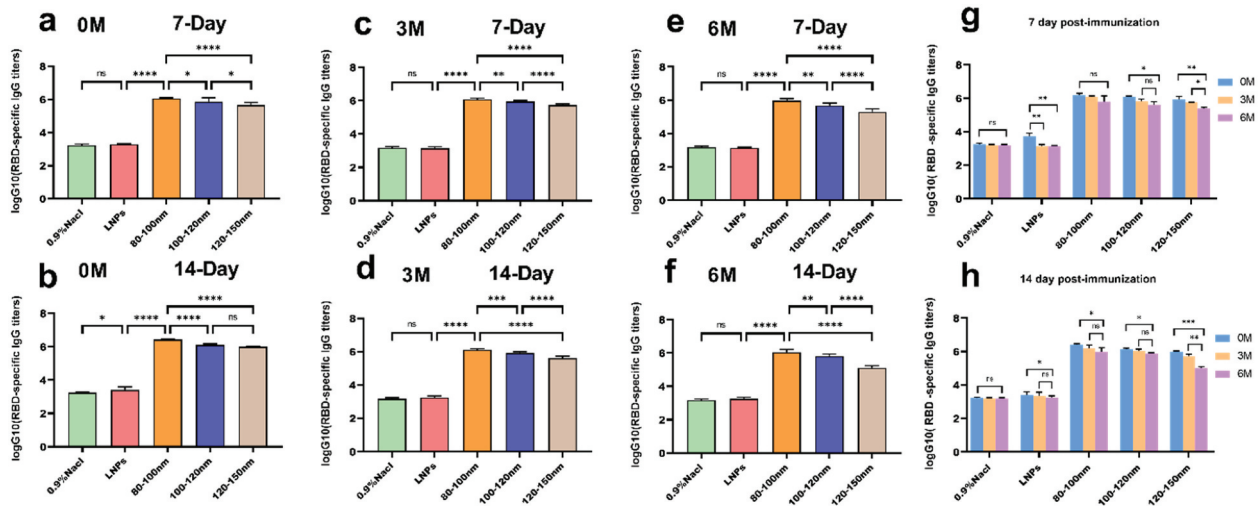


Figure 4. During the entire study, mRNA-LNPs were stored at 4°C, and the samples were stored after 3 and 6 months for evaluation of their biological activity. (a–b) Blood was collected from mice at 7 and 14 days after secondary immunization. (c–d) Blood was collected from mice on days 7 and 14 after secondary immunization when stored for up to 3 months. (e–f) Blood was collected from mice at 7 and 14 days after secondary immunization at 6 months of storage. (g–h) Comparison of serum antibody titers at different intervals for four groups of preparations. Data were analyzed through a two-way ANOVA, Data represent the mean \pm SD ($n = 6$, ^{ns} $p > .05$, * $p < .05$, ** $p < .01$, *** $p < .001$, **** $p < .0001$).

refrigeration) differed significantly among the three vaccine groups and the control group. Notably, the vaccine groups, especially those in the 80–100 nm range, showed a clear advantage in terms of antibody titers (Figure 4(a–c)). This observation remained consistent even after 14 days of secondary immunization (Figure 4(d–f)). The biological activity of the 120–150 nm mRNA-LNPs decreased significantly after storage the preparations at 4°C for 6 months (Figure 4(g,h)). In contrast, the 80–100 nm mRNA-LNPs vaccine did not exhibit any decrease in bioactivity after 3 months of storage at 4°C, and only a slight decrease after being stored for 6 months. The 100–120 nm mRNA-LNPs vaccine showed a slight decrease in activity after 6 months of storage, with an overall 80–100 nm vaccine group showing superior protective properties.

Long-term stability monitoring of mRNA-LNPs freeze at –20°C

To investigate the changes in the stability of vaccines of different sizes when stored at low temperatures, we subjected the four sets of preparations to a cryogenic environment at –20°C. Throughout the test period, the conditions were maintained to be consistent for each batch of preparations. After 3 months of storage, all groups of mRNA-LNPs vaccine preparations exhibited an increased particle size to varying degrees (Figure 5(a)). However, a stable growth plateau was reached within the 3–12 months period. In general, the increase in particle size for the vaccine groups was relatively small when compared to those stored at 4°C. Moreover, the particle size distributions for all four preparation groups remained highly concentrated, with the polydispersity index (PDI) consistently < 0.2 (Figure 5(c)). This observation suggests that the formulations maintained excellent uniform dispersion even after 6 months of storage, and was further supported by the examination of uncoated mRNA nanoparticles (LNPs). Furthermore, the pH and potential trends were smooth, with only a few major changes (Figure 5(b,d)). The encapsulation rates of the four preparation groups varied only minimally, and

their purity levels remained within acceptable limits (Figure 5(e, f)). Collectively, these results highlight the superior dispersion and stability of formulations stored at –20°C compared to those stored at 4°C.

To compare how the content of four lipids (SM-102; DSPC; Cholesterol; mPEG-DMG-2K) of vaccines of different particle sizes change under freezing conditions, we analyzed and compared the individual lipid contents of the four groups preparations stored at –20°C for 0, 3, 6, 9, and 12 months. The contents of four lipids in 60–80 nm LNPs showed a significant decreasing trend (Figure 6(a)). The four lipid contents of 80–100 nm mRNA in the three vaccine groups did not vary significantly (Figure 6(b)). The fractions of cholesterol and DSPC in the 100–120 nm mRNA decreased only a little (Figure 6(c)), while there was a noticeable decrease in cholesterol, DSPC, and SM-102 in the 120–150 nm mRNA group (Figure 6(d)). These results demonstrated that compared to the other two groups, the 80–100 nm mRNA-LNPs vaccine had better stability under –20°C freezing conditions.

In vivo activity of frozen –20°C stored mRNA-LNPs

The levels of IL-4 and IFN- γ cytokines in serum samples were determined at weeks 1, 3, and 5, after the reinforced immunization, by double-antibody sandwich ELISA. (Figure 7(b,c)) At weeks 1 and 3, both IL-4 and IFN- γ levels in serum from the 80–100 nm mRNA group were higher than those in serum from the remaining groups. Meanwhile, the total levels of IL-4 and IFN- γ in the sera of all mRNA-LNPs groups were significantly higher than those in the sera from the 0.9% NaCl group (Figure 7(d,e)). The level of antibodies is an important indicator for evaluating the immune response. Overall, IgG1 and IgG2a levels in the mRNA-LNPs group were significantly higher than those in the 0.9% NaCl group at weeks 1, 2, and 3. The 80–100 nm mRNA vaccines could enhance the production of both Th1-associated IFN- γ and Th2-associated IL-4, better than other groups (Figure 7(f)). The 80–100 nm particle size vaccine led to a significant increase in

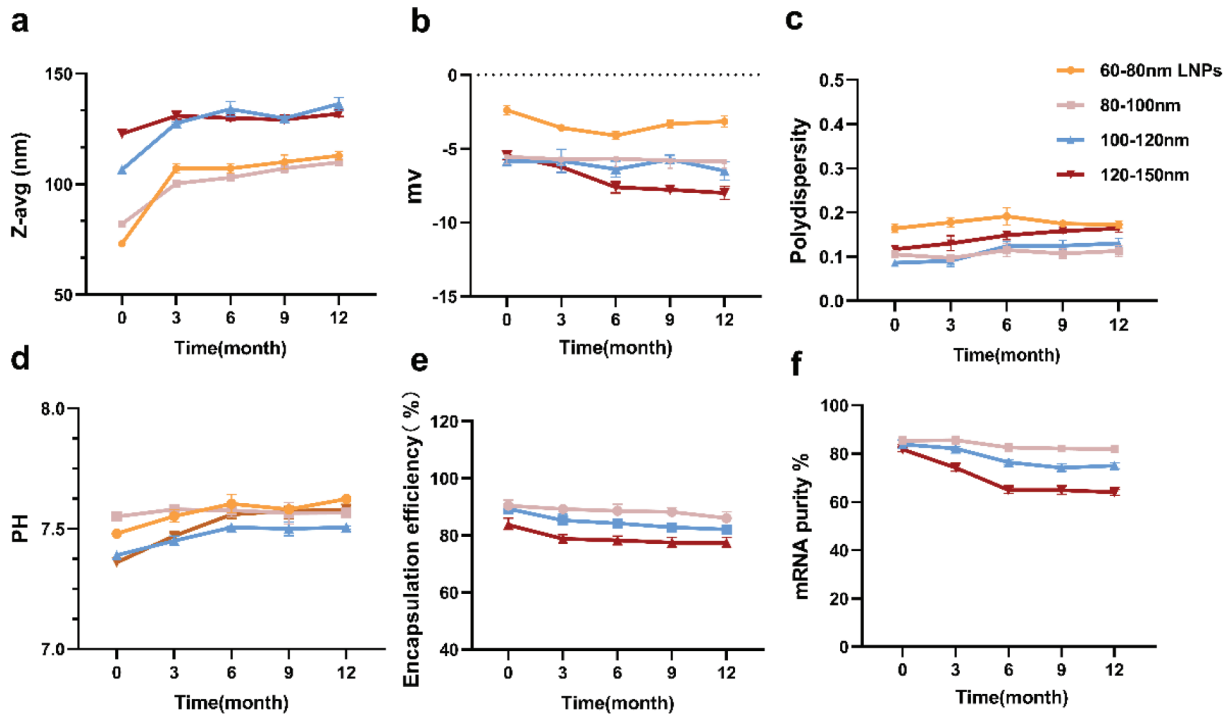


Figure 5. Analytical testing of the physical and chemical characteristics of mRNA-LNPs freeze at -20°C for 0, 3, 6, 9, and 12 months. (a) Particle size, (b) Zeta potential was measured using electrophoretic light scattering, (c) polydispersity was measured by dynamic light scattering, (d) pH value of mRNA-LNPs, (e) mRNA encapsulation was determined by RiboGreen assay, and (f) mRNA purity was assessed by capillary electrophoresis. For (a) (b) (c), and (d), each data point was an aggregate of at least 10 measurements. Error bars are SD.

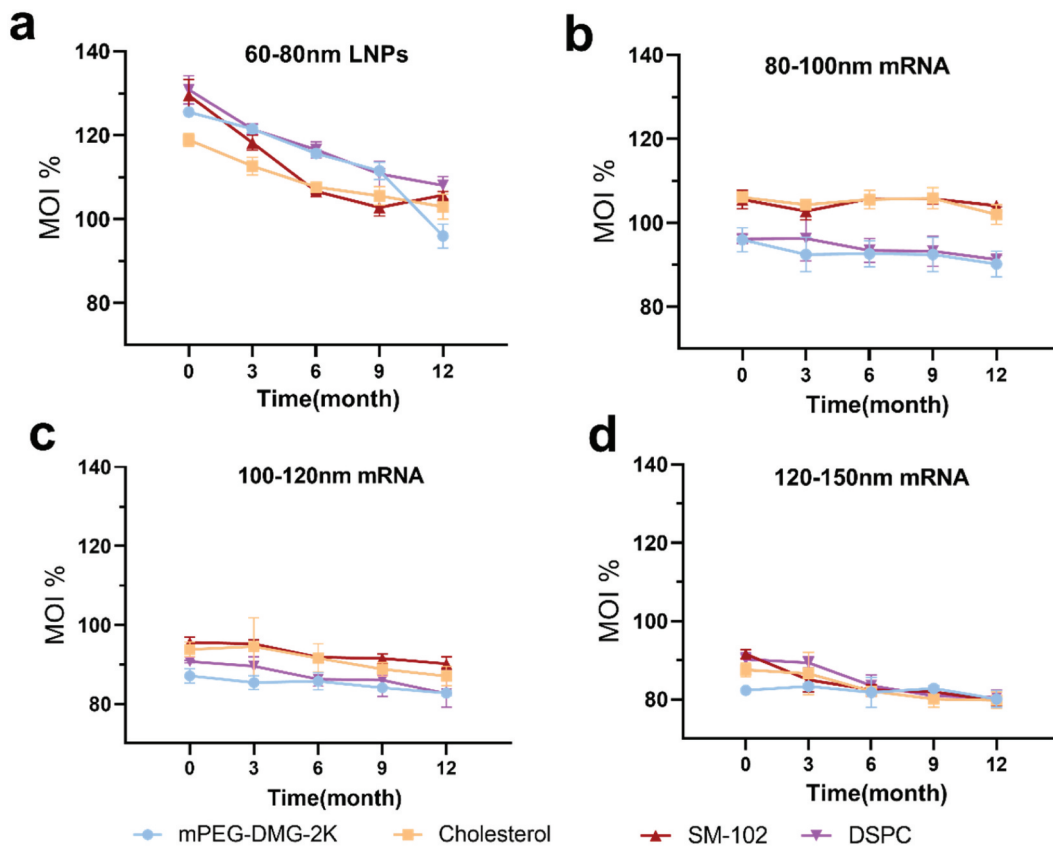


Figure 6. This figure is related to Figure 2. Ultra-high performance liquid chromatography (UHPLC) analysis of individual lipid components of mRNA-LNPs. UHPLC analysis of freshly prepared mRNA-LNPs stored at -20°C for 0, 3, 6, 9, and 12 months. (a) Analysis of four components of 60–80 nm LNPs. (b)(c)(d) Analysis of four lipids from the vaccine set of mRNA-LNPs with different particle sizes (b) 80–100 nm mRNA-LNPs; (c) 100–120 nm mRNA-LNPs; and (d) 120–150 nm mRNA-LNPs. For all panels, analyzes were done in triplicate. Error bars are SD.

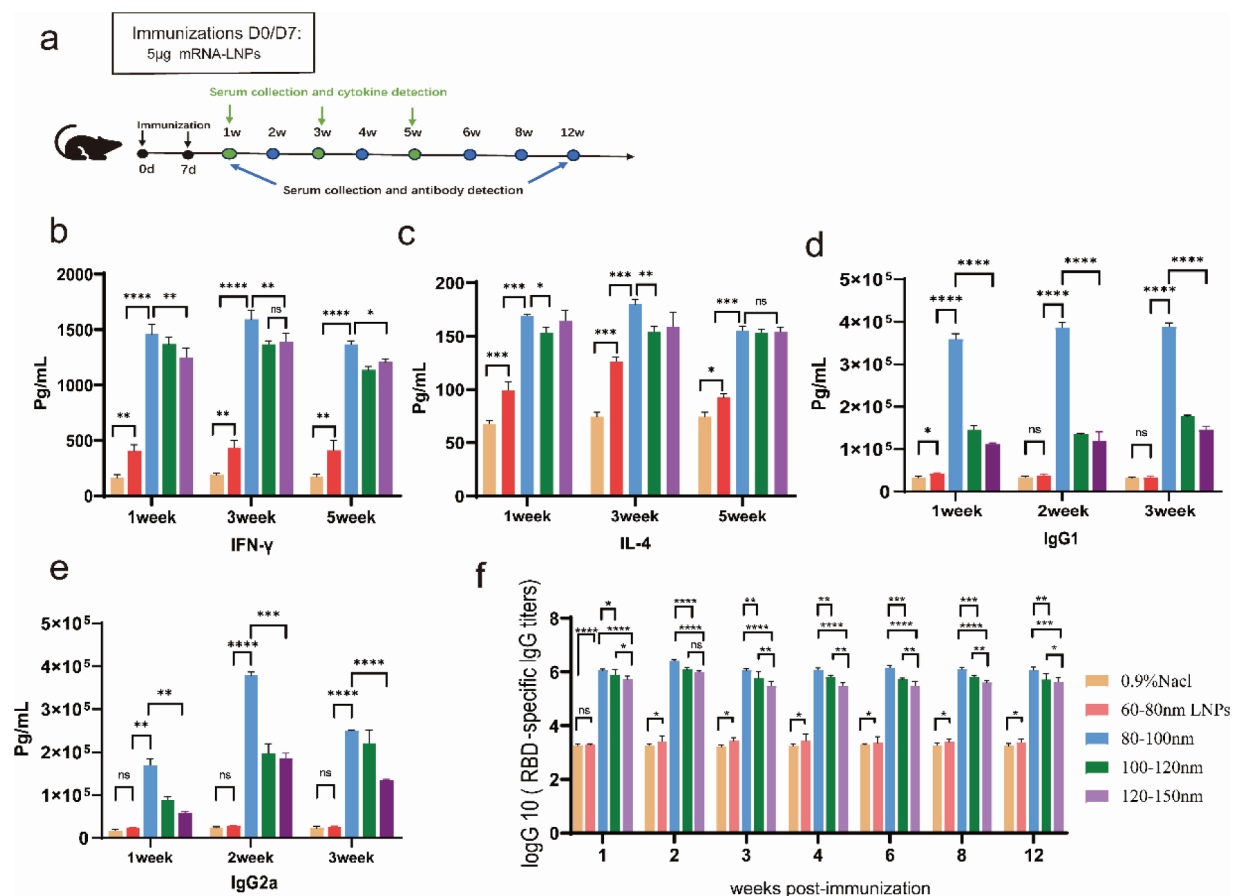


Figure 7. Humoral and cellular immune responses in mice immunized with the mRNA vaccine. Mice were immunized intramuscularly with 5 µg of mRNA vaccine, with a booster of the same dose 7 days after the first vaccination. (a) A schematic diagram of vaccination and sampling in mice. (b,c) Double antibody sandwich assay for determining the levels of IFN-γ and IL-4 in the serum of the mRNA-LNPs immunized mouse. (d,e) Serum levels of total IgG1/IgG2a were measured using ELISA kits. (f) ELISA for the determination of SARS-CoV-2 receptor binding domain-specific IgG antibody titers in immunized animals. Data are shown as mean ± SD, two-way analysis of variance (n = 6; ns $p > .05$, * $p < .05$, ** $p < .01$, *** $p < .001$, **** $p < .0001$).

antibody levels during the second week, followed by a slight decrease, but the expression was always higher compared to the control group. Particularly, all three mRNA vaccines remained strongly bioprotective after 12 weeks. These results suggest that there may be differences in antibody and cytokine levels after immunization between vaccine preparations of different sizes.

Discussion

As mRNA vaccines have taken the lead in late-stage clinical trials to fight the COVID-19 pandemic, challenges surrounding their formulation and stability have become apparent. We reviewed the literature on the approved use and stability of candidate mRNA vaccines, including measures to improve their long-term stability, analytical techniques to monitor their stability, and regulatory guidelines for their characterization and storage stability. We suggest that particle size is an important stability parameter affecting the pharmacokinetics, distribution, safety, and efficacy of vaccines, with appropriate particle size being a focal point in the development of mRNA vaccines; this has the potential to influence the future applications of mRNA vaccines.

The mRNA-LNPs fluid formulations showed an increase in particle size at two different storage temperatures. Under the accelerated storage condition of 4°C, the particle size of the

product exhibited a large increase between 0 and 6 months. Under these conditions, the maximum particle diameter was less than 150 nm (Figure 2(a)). When stored under frozen conditions at -20°C, the particle size of the four groups of formulations showed an increase between 0 and 3 months, remained stable over the next 9 months (Figure 5(a)). Possibly, the observed growth in particle size may be attributed to the Oswald ripening effect,^{23,31} according to which small LNPs with dynamic lipid bilayers might fuse to form larger vesicles during storage. Additionally, the formation of ice crystals during -20°C storage could exert mechanical stress on the LNPs, resulting in size enlargement. These phenomena may collectively contribute to the increase in particle size.^{14,24,2522,32,33} The mPEG-DMG-2K was incorporated into the LNPs to improve their colloidal stability. In early studies of LNPs, polyethylene glycol (PEG) lipids played a crucial role in controlling particle size. This spatial control helped to prevent particle aggregation by stabilizing the LNPs and maintaining their desired size.^{19,2627,34} In our study, the inclusion of the cryoprotectant sucrose notably mitigated the damage to LNPs due to freezing and thawing, thereby minimizing the subsequent impact on the bioactivity of the vaccine.^{27,2835,36} Therefore, we hypothesize that the total volume of particles grows linearly with time at a constant particle number density. This growth can be triggered by thermal drift or any other

activation mechanism but does not affect the diffusion of subsequent mRNA vaccines.^{29,37} This phenomenon can be linked to the PDI dispersibility, (Figure 2(c)) where the PDI index of the three mRNA vaccine groups was still less than 0.2 after 6 months of storage, indicating uniform dispersion in the medium.

The LNPs contain four components. Ionizable amine-based lipids are positively charged in acidic environments and encapsulation of negatively charged mRNAs during particle formation.^{30,38} These lipids also promote the fusion of nuclear endosomes and cytoplasmic release of the payloads once the cells have ingested the LNPs. Saturated phospholipids, such as DSPC, render the LNPs structurally stable and contribute to the overall rigidity of the lipid bilayer. Cholesterol, on the other hand, helps maintain the fluidity of the lipid membrane and enhances the stability and integrity of LNPs. Thus, the amount of lipids can dramatically affect the efficacy and stability of the mRNA vaccine. (Figures 3 and 6) In the present study, the relative integrity of the four lipid components of the LNPs of 80–100 nm mRNA vaccines was maintained regardless of storage at 4°C or –20°C conditions, and these trends are impressive. After storage at 4°C and further storage for 6 months at the same temperature, similar to the other research groups evaluating the stability of encapsulated mRNA LNPs vaccines, we observed a severe degradation of the lipid content in the 120–150 nm vaccine preparations, subsequently leading to a reduction in the biological activity (Figure 4). This emphasizes the importance of the stability of lipid components in vaccine formulation, especially for those stored for long periods.

RNA integrity is a sensitive and critical parameter for stability assays. When preparing mRNA vaccines, it becomes imperative to ensure the usage of highly pure mRNA samples, devoid of contaminants like other RNA, DNA, proteins, and impurities. To assess this, we examined the purity of nucleoside-modified mRNA-LNPs by capillary electrophoresis. Examination of vaccines stored at 4°C revealed a noticeable trend of diminishing mRNA purity. This was particularly evident in 120–150 nm mRNA-LNPs, where the purity of mRNA plummeted from 81% to only 48% (Figure 2(f)). Meanwhile, the vaccine stored at 4°C for 6 months showed a decrease in purity of around 14%–17% for 100–120 nm mRNA and 10% for 80–100 nm mRNA. In contrast, when stored at –20°C, the overall purity for 80–100 nm mRNA dipped only marginally. The purity of 100–120 nm mRNA decreased by about 8%–10%, while 120–150 nm mRNA had a maximum loss of integrity of approximately 20%. Importantly, even at these levels of degradation, in vivo potency remained discernible, only differences that arise include protectiveness against mRNA vaccines of different particle sizes (Figures 4 and 7).

Based on the results mentioned above, we can conclude that freezing the vaccine at –20°C is more suitable for maintaining stability over the long term. Furthermore, the vaccine containing 80–100 nm mRNA-LNPs showed the best stability and protection at both temperature settings. The particle size of a vaccine is closely related to its dispersion and stability in liquid.³⁸ Particles of smaller sizes generally disperse more effectively in solutions, with minimized occurrence of particle precipitation and aggregation.^{31,39} This contributes to maintaining

the uniformity of the vaccine and prevents the settling or aggregation of particles, thereby preserving the physical stability of the formulation.^{32,40} Particle size directly impacts the delivery efficiency of vaccine particles within the body. Some LNPs injected intramuscularly, circulate in the system, leading to their accumulation in the liver and spleen, especially when the LNP size is relatively small. LNPs of larger sizes are more likely to remain at the injection site. Smaller particles are more readily absorbed and transported by immune cells, increasing the effectiveness of the vaccine.^{13,15,33,21,23,41} An appropriate particle size enhances the interaction between vaccine particles and cells, facilitating antigen presentation and immune cell activation.^{34,42} These findings provide valuable considerations for our future research in the development of LNPs delivery systems for vaccines, particularly in the context of particle size selection.

Some researchers believe that the core-shell model offers the most detailed description of mRNA-LNPs, indicating the presence of a surface layer and an affine, isotropic core.^{35,43} They found that 1,2-distearoyl-*sn*-glycero-3-phosphocholine (DSPC) and PEG-lipids, as well as partially ionizable cationic lipids and cholesterol, are located on the surface of the LNPs.^{36,44} Within the core, ionizable cationic lipids, cholesterol, water, and a major portion of mRNA are present. Their study showed that the isotropic LNPs core comprises 24% (volume fraction) water. They propose that mRNA may be located within the water column surrounded by cationic lipids. This would imply that the mRNA is at least partially exposed to the water fraction within the LNPs, leading to its instability when stored under non-frozen conditions. We hypothesized that the 80–100 nm mRNA-LNPs core messenger RNA is relatively minimally exposed to water, retaining its most important portion, as observed by the purity of the mRNA performance. Additionally, the LNPs without encapsulated mRNA exhibited poorer stability in our long-term assay than the mRNA vaccine group, so we suggest that the integrity of the mRNA would largely and simultaneously impede the degradation of the shell LNPs component. Concurrently, liposomes protect mRNA integrity by hiding the interaction of mRNA with serum proteins within the liposome. Thus, the loss of mRNA during long-term storage was minimized, and the stability and efficacy of the vaccine were maintained with long-lasting.

LNPs represent a nonviral leading vector for mRNA delivery. Physicochemical parameters of LNPs, including their size and charge, directly impact their in vivo behavior and, therefore, their cellular internalization.^{37,45} While companies like Moderna and Pfizer/BioNTech have rapidly developed highly effective nucleoside-modified mRNA-LNPs vaccines, issues related to the stability of these vaccines still require further attention.^{38,39,46,47} There have been several reports on the particle size of mRNA-LNPs, but these reports do not sufficiently cover the critical quality attributes and biological effects of these products after extended storage.^{14,40,41,22,48,49} Therefore, we expect to take an important step, particularly in terms of long-term stability and biological activity. We need more studies to fully reveal the impact of size-dependent mRNA delivery. The exact mechanisms explaining these findings and their application in the in vivo environment remain unclear. Therefore, the shape and internal structure of mRNA delivery vectors also need to be further investigated. It will provide

more comprehensive information for subsequent studies of mRNA vaccine particle size.

Acknowledgments

This work was done with contributions from all authors. SR and LX conceived the project and provided discussions. ML and WS performed the experiments and visualized the data. WY and SL contributed to the analysis of the data. All authors have approved the final version of the manuscript. The authors would like to thank all the reviewers who participated in the review, as well as the MJ Editor for providing English editing services during the preparation of this manuscript.

Disclosure statement

No potential conflict of interest was reported by the author(s).

Funding

This study was supported by the Hebei Provincial Key Research and Development Project Program, the Hebei Institute of Medical Device Inspection, North China Pharmaceutical Biotechnology Co. Ltd, and CSPC Zhong Qi Pharmaceutical Technology Co. Ltd.

Ethics statement

The researchers diligently adhered to the “Guidelines for the Care and Use of Laboratory Animals” set forth by the National Research Council’s Committee on Life Sciences. The mouse studies were conducted under protocols approved by the Animal Care and Use Committee of the Hebei Drug and Medical Device Inspection Institute. All animal experiments were carried out following national and local policies and were conducted within facilities accredited by the China Association for Laboratory Animal Care and Accreditation (AAALAC), ensuring the proper care and maintenance of animals.

References

- Hajj KA, Whitehead KA. Tools for translation: non-viral materials for therapeutic mRNA delivery. *Nat Rev Mater*. 2017;2(10):17056. doi:10.1038/natrevmats.2017.56.
- Pardi N, Hogan MJ, Porter FW, Weissman D. mRNA vaccines — a new era in vaccinology. *Nat Rev Drug Discov*. 2018;17(4):261–79. doi:10.1038/nrd.2017.243.
- Erasmus JH, Archer J, Fuerte-Stone J, Khandhar AP, Voigt E, Granger B, Bombardi RG, Govero J, Tan Q, Durnell LA. et al. Intramuscular delivery of replicon RNA encoding ZIKV-117 human monoclonal antibody protects against Zika virus infection. *Mol Ther Methods Clin Dev*. 2020;18:402–14. doi:10.1016/j.omtm.2020.06.011.
- Schoenmaker L, Witzigmann D, Kulkarni JA, Verbeke R, Kersten G, Jiskoot W, Crommelin DJA. mRNA-lipid nanoparticle COVID-19 vaccines: structure and stability. *Int J Pharm*. 2021;601:120586. doi:10.1016/j.ijpharm.2021.120586.
- Hassett KJ, Benenato KE, Jacquinet E, Lee A, Woods A, Yuzhakov O, Himansu S, Deterling J, Geilich BM, Ketova T. et al. Optimization of lipid nanoparticles for intramuscular administration of mRNA vaccines. *Mol Ther Nucleic Acids*. 2019;15:1–11. doi:10.1016/j.omtn.2019.01.013.
- John S, Yuzhakov O, Woods A, Deterling J, Hassett K, Shaw CA, Ciaramella G. Multi-antigenic human cytomegalovirus mRNA vaccines that elicit potent humoral and cell-mediated immunity. *Vaccine*. 2018;36(12):1689–99. doi:10.1016/j.vaccine.2018.01.029.
- Schlake T, Thess A, Fotin-Mlecsek M, Kallen KJ. Developing mRNA-vaccine technologies. *RNA Biol*. 2012;9(11):1319–30. doi:10.4161/rna.22269.
- Sabnis S, Kumarasinghe ES, Salerno T, Mihai C, Ketova T, Senn JJ, Lynn A, Bulychev A, McFadyen I, Chan J. et al. A novel amino lipid series for mRNA delivery: improved endosomal escape and sustained pharmacology and safety in non-human primates. *Mol Ther*. 2018;26(6):1509–19. doi:10.1016/j.yymthe.2018.03.010.
- Kose N, Fox JM, Sapparapu G, Bombardi R, Tennekoon RN, de Silva AD, Elbashir SM, Theisen MA, Humphris-Narayanan E, Ciaramella G. et al. A lipid-encapsulated mRNA encoding a potentially neutralizing human monoclonal antibody protects against chikungunya infection. *Sci Immunol*. 2019;4(35):4. doi:10.1126/sciimmunol.aaw6647.
- Pardi N, Secreto AJ, Shan X, Debonera F, Glover J, Yi Y, Muramatsu H, Ni H, Mui BL, Tam YK. et al. Administration of nucleoside-modified mRNA encoding broadly neutralizing antibody protects humanized mice from HIV-1 challenge. *Nat Commun*. 2017;8(1):14630. doi:10.1038/ncomms14630.
- Van Hoecke L, Verbeke R, De Vlioger D, Dewitte H, Roose K, Van Nevel S, Krysko O, Bachert C, Schepens B, Lentacker I. et al. mRNA encoding a bispecific single domain antibody construct protects against influenza A virus infection in mice. *Mol Ther Nucleic Acids*. 2020;20:777–87. doi:10.1016/j.omtn.2020.04.015.
- Baden LR, El Sahly HM, Essink B, Kotloff K, Frey S, Novak R, Diemert D, Spector SA, Rouphael N, Creech CB. et al. Efficacy and safety of the mRNA-1273 SARS-CoV-2 vaccine. *N Engl J Med*. 2021;384(5):403–16. doi:10.1056/NEJMoa2035389.
- Deng YQ, Zhang NN, Zhang YF, Zhong X, Xu S, Qiu HY, Wang T-C, Zhao H, Zhou C, Zu S-L. et al. Lipid nanoparticle-encapsulated mRNA antibody provides long-term protection against SARS-CoV-2 in mice and hamsters. *Cell Res*. 2022;32(4):375–82. doi:10.1038/s41422-022-00630-0.
- Muramatsu H, Lam K, Bajusz C, Laczko D, Kariko K, Schreiner P, Martin A, Lutwyche P, Heyes J, Pardi N. et al. Lyophilization provides long-term stability for a lipid nanoparticle-formulated, nucleoside-modified mRNA vaccine. *Mol Ther*. 2022;30(5):1941–51. doi:10.1016/j.yymthe.2022.02.001.
- Howard GP, Verma G, Ke X, Thayer WM, Hamerly T, Baxter VK, Lee JE, Dinglasan RR, Mao H-Q. Critical size limit of biodegradable nanoparticles for enhanced lymph node trafficking and paracortex penetration. *Nano Res*. 2019;12(4):837–44. doi:10.1007/s12274-019-2301-3.
- Crommelin DJA, Anchordoquy TJ, Volkin DB, Jiskoot W, Mastrobattista E. Addressing the cold reality of mRNA vaccine stability. *J Pharm Sci*. 2021;110(3):997–1001. doi:10.1016/j.xphs.2020.12.006.
- Oude Blenke E, Örnkvist E, Schöneich C, Nilsson GA, Volkin DB, Mastrobattista E, Almarsson Ö, Crommelin DJA. The storage and in-use stability of mRNA vaccines and therapeutics: not a cold case. *J Pharm Sci*. 2023;112(2):386–403. doi:10.1016/j.xphs.2022.11.001.
- Wang T, Sung TC, Yu T, Lin HY, Chen YH, Zhu ZW, Gong J, Pan J, Higuchi A. Next-generation materials for RNA-lipid nanoparticles: lyophilization and targeted transfection. *J Mater Chem B*. 2023;11(23):5083–93. doi:10.1039/D3TB00308F.
- Poveda C, Biter AB, Bottazzi ME, Strych U. Establishing preferred product characterization for the evaluation of RNA vaccine antigens. *Vaccines*. 2019;7(4):7. doi:10.3390/vaccines7040131.
- Fan Y, Marioli M, Zhang K. Analytical characterization of liposomes and other lipid nanoparticles for drug delivery. *J Pharm Biomed Anal*. 2021;192:113642. doi:10.1016/j.jpba.2020.113642.
- Kim J, Eygeris Y, Gupta M, Sahay G. Self-assembled mRNA vaccines. *Adv Drug Deliv Rev*. 2021;170:83–112. doi:10.1016/j.addr.2020.12.014.
- Suzuki Y, Hyodo K, Tanaka Y, Ishihara H. siRNA-lipid nanoparticles with long-term storage stability facilitate potent gene-silencing in vivo. *J Control Release*. 2015;220:44–50. doi:10.1016/j.jconrel.2015.10.024.

23. Gindy ME, Feuston B, Glass A, Arrington L, Haas RM, Schariter J, Stirdivant SM. Stabilization of Ostwald ripening in low molecular weight amino lipid nanoparticles for systemic delivery of siRNA therapeutics. *Mol Pharm.* 2014;11(11):4143–53. doi:10.1021/mp500367k.
24. Suzuki Y, Miyazaki T, Muto H, Kubara K, Mukai Y, Watari R, Sato S, Kondo K, Tsukumo S-I, Yasutomo K. et al. Design and lyophilization of lipid nanoparticles for mRNA vaccine and its robust immune response in mice and nonhuman primates. *Mol Ther Nucleic Acids.* 2022;30:226–40. doi:10.1016/j.omtn.2022.09.017.
25. Wang Y, Grainger DW. Lyophilized liposome-based parenteral drug development: reviewing complex product design strategies and current regulatory environments. *Adv Drug Deliv Rev.* 2019;151–152:56–71. doi:10.1016/j.addr.2019.03.003.
26. Zhao P, Hou X, Yan J, Du S, Xue Y, Li W, Xiang G, Dong Y. Long-term storage of lipid-like nanoparticles for mRNA delivery. *Bioact Mater.* 2020;5(2):358–63. doi:10.1016/j.bioactmat.2020.03.001.
27. Hald Albertsen C, Kulkarni JA, Witzigmann D, Lind M, Petersson K, Simonsen JB. The role of lipid components in lipid nanoparticles for vaccines and gene therapy. *Adv Drug Deliv Rev.* 2022;188:114416. doi:10.1016/j.addr.2022.114416.
28. Franzé S, Selmin F, Samaritani E, Minghetti P, Cilurzo F. Lyophilization of liposomal formulations: still necessary, still challenging. *Pharmaceutics.* 2018;10(3):10. doi:10.3390/pharmaceutics10030139.
29. Jakubek ZJ, Chen S, Zaifman J, Tam YYC, Zou S. Lipid nanoparticle and liposome reference materials: assessment of size homogeneity and long-term $-70\text{ }^{\circ}\text{C}$ and $4\text{ }^{\circ}\text{C}$ Storage Stability. *Langmuir.* 2023;39(7):2509–19. doi:10.1021/acs.langmuir.2c02657.
30. Lamoot A, Lammens J, De Lombaerde E, Zhong Z, Gontsarik M, Chen Y, De Beer TRM, De Geest BG. Successful batch and continuous lyophilization of mRNA LNP formulations depend on cryoprotectants and ionizable lipids. *Biomater Sci.* 2023;11(12):4327–34. doi:10.1039/D2BM02031A.
31. Pardi N, Carreno JM, O'Dell G, Tan J, Bajusz C, Muramatsu H, Rijnink W, Strohmeier S, Loganathan M, Bielak D. et al. Development of a pentavalent broadly protective nucleoside-modified mRNA vaccine against influenza B viruses. *Nat Commun.* 2022;13(1):4677. doi:10.1038/s41467-022-32149-8.
32. Costa VG, Costa SM, Saramago M, Cunha MV, Arraiano CM, Viegas SC, Matos RG. Developing new tools to fight human pathogens: a journey through the advances in RNA technologies. *Microorganisms.* 2022;10(11):10. doi:10.3390/microorganisms10112303.
33. Foged C, Brodin B, Frokjaer S, Sundblad A. Particle size and surface charge affect particle uptake by human dendritic cells in an in vitro model. *Int J Pharm.* 2005;298(2):315–22. doi:10.1016/j.ijpharm.2005.03.035.
34. Gao X, Liu N, Wang Z, Gao J, Zhang H, Li M, Du Y, Gao X, Zheng A. Development and optimization of chitosan nanoparticle-based intranasal vaccine carrier. *Molecules.* 2021;27(1):27. doi:10.3390/molecules27010204.
35. Viger-Gravel J, Schantz A, Pinon AC, Rossini AJ, Schantz S, Emsley L. Structure of lipid nanoparticles containing siRNA or mRNA by dynamic nuclear polarization-enhanced NMR spectroscopy. *J Phys Chem B.* 2018;122(7):2073–81. doi:10.1021/acs.jpcc.7b10795.
36. Yanez Arteta M, Kjellman T, Bartesaghi S, Wallin S, Wu X, Kvist AJ, Dabkowska A, Székely N, Radulescu A, Bergenholtz J. et al. Successful reprogramming of cellular protein production through mRNA delivered by functionalized lipid nanoparticles. *Proc Natl Acad Sci U S A.* 2018;115(15):E3351–e60. doi:10.1073/pnas.1720542115.
37. Malburet C, Leclercq L, Cotte JF, Thiebaud J, Bazin E, Garinot M, Cottet H. Size and charge characterization of lipid nanoparticles for mRNA vaccines. *Anal Chem.* 2022;94(11):4677–85. doi:10.1021/acs.analchem.1c04778.
38. Skowronski DM, De Serres G. Safety and efficacy of the BNT162b2 mRNA Covid-19 vaccine. *N Engl J Med.* 2021;384:1576–7.
39. Hogan MJ, Pardi N. mRNA vaccines in the COVID-19 pandemic and beyond. *Annu Rev Med.* 2022;73(1):17–39. doi:10.1146/annurev-med-042420-112725.
40. Meulewaeter S, Nuytten G, Cheng MHY, De Smedt SC, Cullis PR, De Beer T, Lentacker I, Verbeke R. Continuous freeze-drying of messenger RNA lipid nanoparticles enables storage at higher temperatures. *J Control Release.* 2023;357:149–60. doi:10.1016/j.jconrel.2023.03.039.
41. Muramatsu H, Lam K, Bajusz C, Laczko D, Karikó K, Schreiner P, Martin A, Lutwyche P, Heyes J, Pardi N. et al. Lyophilization provides long-term stability for a lipid nanoparticle-formulated, nucleoside-modified mRNA vaccine. *Mol Ther.* 2022;30(5):1941–51. doi:10.1016/j.ymthe.2022.02.001.